



Note

Two coordination modes of TCNE in the ruthenium amidinates: The first example providing experimental evidence for κ^1 -N to η^2 -C rearrangementHideo Kondo^b, Takashi Sue^b, Akira Kageyama^b, Yoshitaka Yamaguchi^b, Yusuke Sunada^a, Hideo Nagashima^{a,b,*}^a Division of Applied Molecular Chemistry and Institute for Materials Chemistry and Engineering, Kyushu University, Kasuga, Fukuoka 816-8580, Japan^b Graduate School of Engineering Sciences, Kyushu University, Kasuga, Fukuoka 816-8580, Japan

ARTICLE INFO

Article history:

Received 27 September 2008

Received in revised form 9 December 2008

Accepted 12 December 2008

Available online 25 December 2008

Keywords:

TCNE

Ruthenium amidinate

Rearrangement

ABSTRACT

Reactions of $\text{Cp}^*\text{Ru}(\kappa^2\text{-N(R)}=\text{C(R')NR})$ (**1a**; R = ⁱPr, R' = Me, **1b**; R = ^tBu, R' = Ph) with TCNE initially give dark green colored intermediary species, which are readily converted to brown colored " η^2 -C" coordination complexes, $\text{Cp}^*\text{Ru}(\kappa^2\text{-N(R)}=\text{C(R')NR})(\eta^2\text{-TCNE})$ (**3a**; R = ⁱPr, R' = Me, **3b**; R = ^tBu, R' = Ph). These " η^2 -C" complexes are characterized by spectroscopy and crystallography. A stable ruthenium amidinate having a " κ^1 -N"-coordinated TCNE, $\text{Cp}^*\text{Ru}(\kappa^2\text{-N}^t\text{Bu}=\text{C}(\text{Mes})\text{N}^i\text{Bu})(\kappa^1(\text{N})\text{-TCNE})$ (**2c**), is synthesized by treatment of $\text{Cp}^*\text{Ru}(\kappa^2\text{-N}^t\text{Bu}=\text{C}(\text{Mes})\text{N}^i\text{Bu})$ (**1c**) with TCNE, the structure of which is unequivocally confirmed by X-ray structure determination and the charge transfer nature is supported by ESR analysis. Close analogy in IR and UV–Vis spectroscopy of **2c** with the dark green colored intermediary species formed from **1b** suggests that this is " κ^1 -N" ruthenium amidinate, which is rearranged to the " η^2 -C" complex **3b**.

© 2008 Elsevier B.V. All rights reserved.

1. Introduction

Tetracyanoethylene (TCNE) is a typical strongly electron-withdrawing alkene, and exhibits strong affinity to electron-donating organometallic species [1]. Coordination of TCNE to coordinatively unsaturated organometallic species often results in formation of the corresponding η^2 -TCNE complexes, in which central carbons of TCNE are bound to the metal center [1,2]. The electron-withdrawing property of TCNE leads to donation of d-electrons from occupied orbitals of metallic species to LUMO of TCNE, giving η^2 -TCNE complexes (the " η^2 -C" complex, Chart 1A) with a structure close to "metallacyclopropane extreme". In contrast, there have been several reported examples of the complexes, in which a $\text{N}\equiv\text{C}$ moiety of TCNE is coordinated to the metal center to form $\kappa^1\text{-NC}(\text{CN})\text{C}=\text{CCN}_2$ compounds [3,4]. Since TCNE is a strong electron acceptor, these formed $\kappa^1\text{-NC}(\text{CN})\text{C}=\text{C}(\text{CN})_2$ compounds (the " κ^1 -N" complex, Chart 1B) are normally charge-transfer species, in which a cation radical is located on the metal center, whereas an anion radical exists on a carbon of the " κ^1 -N" TCNE ligand. Two metallic species, A and B, are structural isomers, and there is a possible interconversion pathway between A and B. In fact, there are some examples of the electron-transfer-, photo-, or thermally-induced isomerization from A to B [5]. However, the

stepwise auto-isomerization of B to A has never been reported to our best knowledge.

As reported earlier, we have synthesized and characterized isolable 16-electron organoruthenium amidinates, $\text{Cp}^*\text{Ru}(\kappa^2\text{-amidinate})$ (**1**) [6,7]. The coordinatively unsaturated nature of **1** results in facile reaction with TCNE, leading to isolation of $\text{Cp}^*\text{Ru}(\eta^2\text{-TCNE})(\kappa^2\text{-amidinate})$ having the " η^2 -C" structure [6]. Interestingly, impressive color change of the solution was observed during the reaction. In a typical example, color of the reaction mixture of $\text{Cp}^*\text{Ru}(\kappa^2\text{-N}^i\text{Pr}=\text{C}(\text{Me})\text{N}^i\text{Pr})$ (**1a**) and TCNE is dark purple \rightarrow dark green \rightarrow brown. The dark purple color species corresponds to **1a**, whereas the brown is the color of $\text{Cp}^*\text{Ru}(\eta^2\text{-TCNE})(\kappa^2\text{-N}^i\text{Pr}=\text{C}(\text{Me})\text{N}^i\text{Pr})$ (**3a**), which was isolated and characterized. The dark green species formed from **1a** is unstable, and has not been characterized yet. In this paper, we wish to report the synthesis of the dark green colored species with longer lifetime, which was obtained by the reaction of two derivatives of $\text{Cp}^*\text{Ru}(\kappa^2\text{-N}^t\text{Bu}=\text{C}(\text{R})\text{N}^i\text{Bu})$ (**1b**; R = Ph, **1c**; R = mesityl) with TCNE. The results suggest that charge transfer " κ^1 -N isomer" of $\text{Cp}^*\text{Ru}(\kappa\text{-TCNE})(\kappa^2\text{-amidinate})$ is involved in the reaction of **1a** with TCNE to form **3a** with the " η^2 -C" coordination mode.

2. Results and discussion

We previously became aware that treatment of a coordinatively unsaturated 16e ruthenium amidinate, $\text{Cp}^*\text{Ru}(\kappa^2\text{-N}^i\text{Pr}=\text{C}(\text{Me})\text{-N}^i\text{Pr})$ (**1a**), with 1 equiv. of TCNE gives a dark green species, which

* Corresponding author. Address: Division of Applied Molecular Chemistry and Institute for Materials Chemistry and Engineering, Kyushu University, Kasuga, Fukuoka 816-8580, Japan.

E-mail address: nagasima@cm.kyushu-u.ac.jp (H. Nagashima).

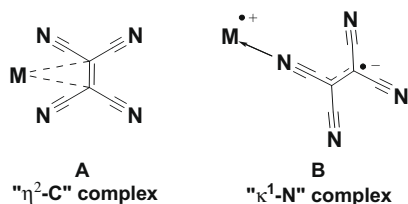


Chart 1.

is converted to brown $\text{Cp}^*\text{Ru}(\kappa^2\text{-}i\text{PrN}=\text{C}(\text{Me})\text{N}^i\text{Pr})(\eta^2\text{-TCNE})$ (**3a**) within one minute. Elaboration to capture a dark green species with longer life time resulted in discovery that $\text{Cp}^*\text{Ru}(\kappa^2\text{-N}(\text{tBu})=\text{C}(\text{Ph})\text{N}^t\text{Bu})$ (**1b**) reacted with TCNE to give a dark green species stable in a solution for ca. 1 h. The color of the solution gradually turned brown, and after 6 h, brown colored $\text{Cp}^*\text{Ru}(\kappa^2\text{-N}(\text{tBu})=\text{C}(\text{Me})\text{N}^t\text{Bu})(\eta^2\text{-TCNE})$ (**3b**) was formed exclusively. Characterization of two “ $\eta^2\text{-C}$ ” isomers, **3a** and **3b**, was carried out by spectroscopic methods as well as determination of the X-ray structure of **3a**. Typically, a ^{13}C resonance due to the olefinic carbon of TCNE appeared at δ 20.7 (**3a**) and δ 18.8 (**3b**), respectively, which are significantly shifted to upfield compared with the uncoordinated TCNE (δ 80.3). IR absorptions of $\nu_{\text{C}=\text{N}}$ appeared around 2226, 2209 cm^{-1} for **3a** and 2229, 2211 cm^{-1} for **3b**, which are shifted to a lower wavenumber than those of the uncoordinated TCNE (2262, 2228, 2214 cm^{-1}) [8]. The X-ray diffraction analysis of **3a** revealed that the ruthenium center adopts the three-legged piano-stool structure with two nitrogen atoms of amidinate ligand and the center of the C=C bond of TCNE [6]. It is noteworthy that significant elongation of the carbon-carbon bond length was observed [**3a**: C=C 1.499(6) Å; uncoordinated TCNE: C=C 1.344(3) Å] [8], which strongly suggests that the coordination mode of TCNE is “metallacyclopropane extreme”, and the formal oxidation state of the ruthenium center is Ru(IV). The dark green colored intermediary species was monitored by UV–Vis spectra of the reaction of **1b** with TCNE in THF, which showed absorptions at 635–641 ($\epsilon = 698 \text{ M}^{-1} \text{ cm}^{-1}$) and 831 ($\epsilon = 627 \text{ M}^{-1} \text{ cm}^{-1}$) nm and are characteristic of charge-transfer complexes [4g,5a,5c]. Fig. 1 shows time-dependent UV–Vis spectral changes for formation of **3b**, indicating the presence of the intermediary dark green¹ complex **2b** during the reaction (vide infra). IR spectrum of the intermediary species showed three ν_{CN} absorptions at 2195, 2154, and 2116 cm^{-1} , suggesting the unsymmetrical coordination of TCNE to the metal center, which is often seen in the charge transfer metal complexes of TCNE [3,4,8].

Elaboration to isolate the dark green colored species as a stable form was successful, when the mesityl group was introduced to the central carbon of the amidinate ligand. The ruthenium amidinate, $\text{Cp}^*\text{Ru}(\kappa^2\text{-N}(\text{tBu})=\text{C}(\text{Mes})\text{N}^t\text{Bu})$ (**1c**), was synthesized in 98% yield as dark purple crystals by treatment of $[\text{Cp}^*\text{RuCl}]_4$ with 0.25 equiv. of $\text{Li}(\text{N}(\text{tBu})=\text{C}(\text{Mes})\text{N}^t\text{Bu})$ in THF at 60 °C for 4 h (Scheme 1). The product **1c** was unequivocally characterized by X-ray diffraction analysis, NMR spectroscopy, and elemental analysis. The molecular structure of **1c** was established by X-ray study and Fig. 2 shows the ORTEP view of **1c**, the selected bond distances and angles of **1c** are listed in Table 1. The crystallographic data is listed in Table 2. The Ru atom adopts the two-legged piano-stool structure which is often seen in the molecular structure of the coordinatively unsaturated 16e Ru mononuclear species [9]. The angle θ (177.98(3)°) of **1c** which is defined in Fig. 3 is close to 180°, which is typically seen in the coordinatively uncoordinated ruthenium amidinate [7d]. The amidinate ligand is bent, and the dihedral angle δ defined by

the N(1)–Ru–N(2) plane and the N(1)–C(11)–N(2) plane (Fig. 3) is 21.5°, which is much more acute compared with that of the (central)C–Ph analogue **1b** (48.9°). The bond length of Ru–C(1) in **1c** (2.422(3) Å) is ca. 0.1 Å longer than that in complex **1b** (2.336 Å). This significantly small dihedral angle δ and lengthening of the Ru–C(1) bond are caused by steric repulsion between the methyl groups of the Cp* ligand and an *ortho*-methyl moiety of the mesityl group, which provides a smaller coordination sphere around the ruthenium center than that of the other ruthenium amidinates, **1a** and **1b**. ^1H and ^{13}C NMR spectrum of **1c** showed two signals at $\delta_{\text{H}} = 2.20$ and 2.21 (singlet) with an integral ratio of 3:6 and $\delta_{\text{C}} = 21.1$ and 22.7 ppm, which are assignable to *para*- and *ortho*-methyl moieties of the mesityl group, respectively. On the basis of the crystal structure, the two *ortho* methyl signals should be magnetically inequivalent; however, the dynamic process shown in Scheme 2 was not frozen to give a single peak (singlet) which is derived from the *o*-mesityl group even at –90 °C. Methyl signals due to the tBu and Cp* moiety appeared at 1.16 and 1.69 ppm, respectively, in the integral ratio of 18:15.

Treatment of **1c** with TCNE resulted in instant color change from dark purple to dark green as seen in the reaction of **1b** with TCNE, however, the solution remained a dark green color even after 24 h (Scheme 3). From this solution, a product having the “ $\kappa^1\text{-N}$ ” structure, $\text{Cp}^*\text{Ru}(\kappa^2\text{-N}(\text{tBu})=\text{C}(\text{Mes})\text{N}^t\text{Bu})(\kappa^1(\text{N})\text{-TCNE})$ (**2c**) was isolated as dark green crystals in 94% yield.

The molecular structure of **2c** was determined by crystallography. The ORTEP drawing (Fig. 4) revealed that the ligand arrangement around the ruthenium has a coordinatively saturated three-legged piano-stool structure. As shown in the supporting information, TCNE moiety is rotationally disordered with the occupancy of 0.7 and 0.3, and one of the TCNE moieties is depicted in Fig. 4. The angle θ of 142.85 (5)° is in the normal range of θ of known coordinatively saturated ruthenium amidinates [6,7c,7h]. The UV spectrum of **2c** is similar to that of an intermediary species **2b** observed in the reaction of **1b** with TCNE, giving two absorptions at 632 ($\epsilon = 698 \text{ M}^{-1} \text{ cm}^{-1}$) and 850 ($\epsilon = 627 \text{ M}^{-1} \text{ cm}^{-1}$) nm (Fig. 5). IR spectrum of **2c** is also similar to that of **2b**, giving three ν_{CN} absorptions at 2215, 2192, and 2110 cm^{-1} . The complex **2c** is diamagnetic [10], and ^1H and ^{13}C NMR spectrum of **2c** show two signals at $\delta_{\text{H}} = 1.86$ and 2.50 (singlet), and $\delta_{\text{C}} = 20.9$ and 25.4 ppm, which are assignable to two inequivalent *ortho*-methyl moieties of the mesityl group. Unfortunately, the signals derived from the C≡N and central C–C moieties were not detected due to the low solubility of **2c**. The charge transfer nature of **2c** is evidenced by ESR signals at $g = 2.00021$ with the ^{14}N coupling, which can be interpreted as the oxidation state of ruthenium being III and location of an anion radical on a carbon of the TCNE ligand.

All of these results strongly suggest that coordination of the TCNE to the coordinatively unsaturated 16e Ru(II) amidinates proceeded stepwise; a C≡N group of TCNE is bonded to the ruthenium center with a $\kappa^1\text{-NCC}(\text{CN})=\text{C}(\text{CN})_2$ mode (the “ $\kappa^1\text{-N}$ ” isomer); the coordination accompanied by transfer of an electron from the Ru(II) center to the TCNE ligand, giving Ru(III) and $\text{TCNE}^{\cdot-}$. The transfer of another electron from the Ru(III) center to the coordinated $\text{TCNE}^{\cdot-}$ results in isomerization from the “ $\kappa^1\text{-N}$ ” isomer to $\text{Cp}^*\text{Ru}(\eta^2\text{-TCNE})(\kappa^2\text{-amidinate})$ (the “ $\eta^2\text{-C}$ ” isomer). The rearrangement from the “ $\kappa^1\text{-N}$ ” isomer to the “ $\eta^2\text{-C}$ ” isomer may involve dissociation and recoordination of TCNE. The “ $\eta^2\text{-C}$ ” isomer has a structure close to ruthenacyclopropane extreme, of which formal oxidation state is Ru(IV). A key experimental result to support this mechanism is isolation of **2c** with the “ $\kappa^1\text{-N}$ ” structure, of which spectroscopic features (UV, IR) are similar to those of **2b**. Although **2c** did not isomerize to the “ $\eta^2\text{-C}$ ” isomer, the “ $\kappa^1\text{-N}$ ” isomer of **2b** is not very stable and slowly converted to the corresponding “ $\eta^2\text{-C}$ ” isomer. It is dependent on the steric circumstances around the ruthenium center how easy the isomer-

¹ For interpretation of color in Fig. 1, the reader is referred to the web version of this article.

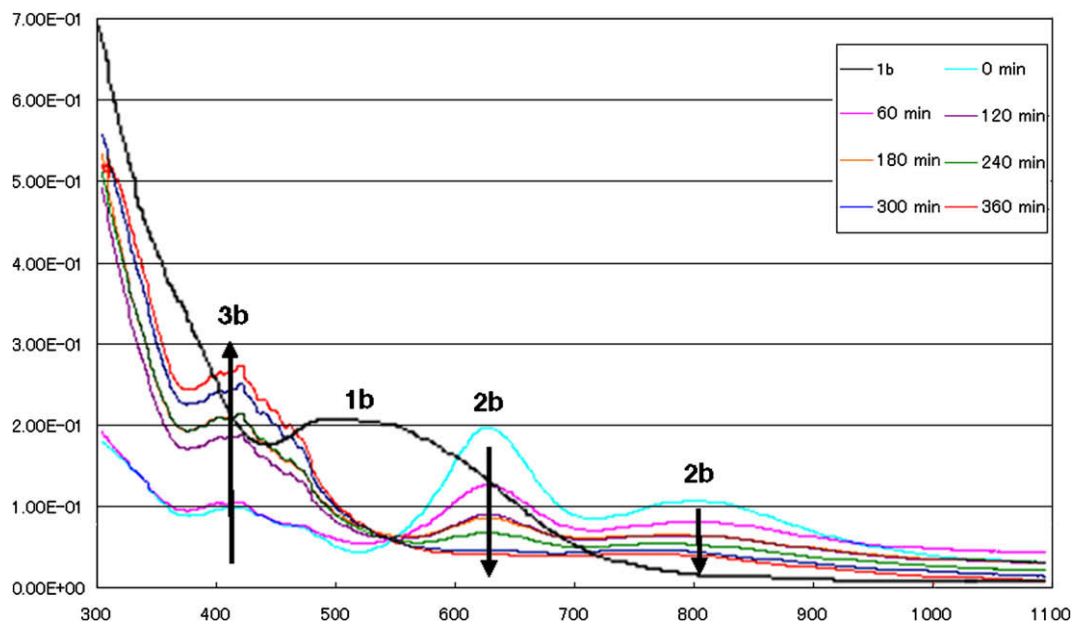


Fig. 1. Time-dependent UV-Vis spectral changes for **1b** → **2b** → **3b**.

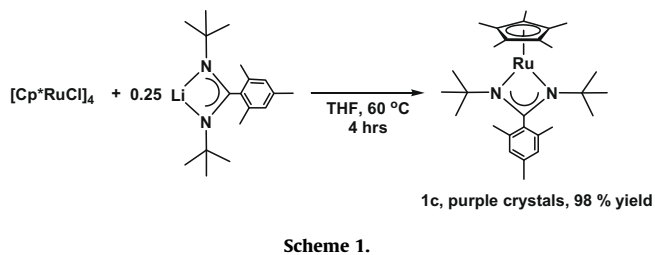


Table 1
Representative bond lengths and angles for **1c** and **2c**.

	1c	2c
<i>Bond lengths (Å)</i>		
Ru–N(1)	2.101(3)	2.078(4)
Ru–N(2)	2.084(3)	2.104(3)
Ru–C(1)	2.422(3)	–
<i>Bond angles (°)</i>		
N(1)–Ru–N(2)	63.00(14)	62.2(2)
Ru–N(1)–C(1)	87.1(2)	81.73(6)
Ru–N(2)–C(1)	86.9(2)	95.5(3)
N(1)–C(1)–N(2)	110.3(3)	107.6(4)

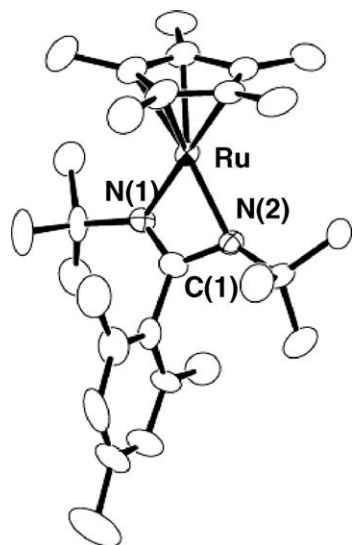


Fig. 2. The molecular structure of **1c** with 50% probability ellipsoids. The hydrogen atoms were omitted for clarity.

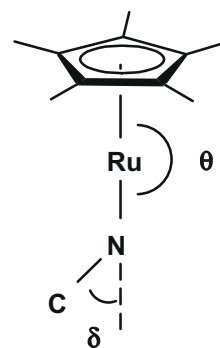
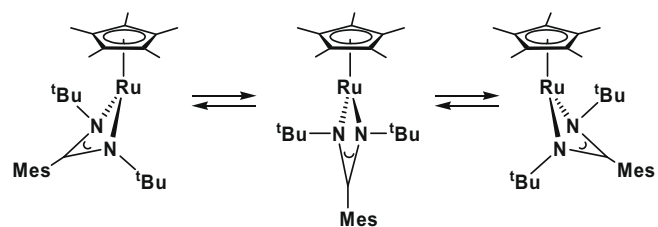
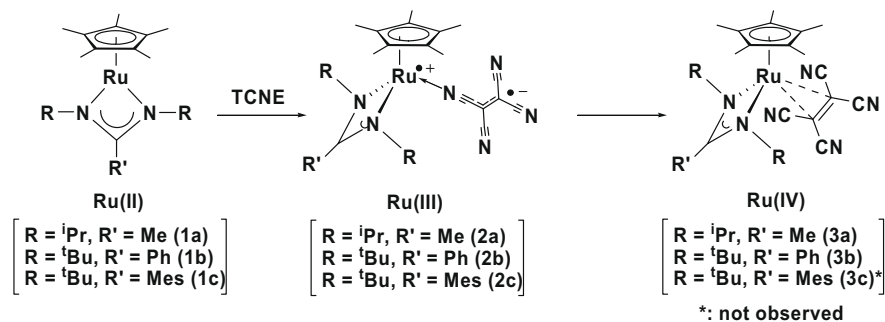


Fig. 3. Definition of the angle θ and δ .



Scheme 2.



Scheme 3.

Table 2
Crystallographic data for **1c** and **2c**.

	1c	2c
Empirical formula	C ₂₈ H ₄₄ N ₂ Ru	C ₄₁ H ₄₉ N ₆ Ru
Formula weight	509.74	726.95
Crystal system	Triclinic	Monoclinic
Lattice type	Primitive	C-centered
Space group	P1 (#2)	C2/c (#15)
a (Å)	10.7937(10)	34.150(14)
b (Å)	13.3321(13)	11.857(4)
c (Å)	9.6704(9)	19.085(8)
α (°)	104.141(5)	90
β (°)	91.762(3)	100.4000(9)
γ (°)	80.126(4)	90
Volume (Å ³)	1329.3(2)	6576(3)
Z value	2	8
D _{calc} (g/cm ³)	1.273	1.295
F(000)	540.00	3048.00
Crystal color, habit	Dark purple, platelet	Dark green, platelet
Crystal dimensions, mm	0.20 × 0.15 × 0.10	0.19 × 0.12 × 0.03
Number of observations (all reflections)	5781	8527
Number of variables	324	474
Reflection/parameter ratio	17.84	17.99
R (all reflections)	0.0607	0.1118
R ₁ (I > 2σ(I)) ^a	0.0578	0.0856
wR ₂ (all reflections) ^b	0.2182	0.2666
Goodness-of-fit	0.999	1.000
Maximum shift/error in final cycle	0.000	0.000
Maximum peak in final difference Map, e-/Å ³	1.66	4.52
Minimum peak in final difference Map, e-/Å ³	-1.78	-1.72

^a $R_1 = \frac{\sum |F_0| - |F_c|}{\sum |F_0|}$.

^b $wR_2 = \left[\frac{\sum (w(F_0^2 - F_c^2)^2)}{\sum (w(F_0^2)^2)} \right]^{1/2}$.

ization is from the “κ¹-N” isomer to the “η²-C” isomer. The smallest δ of **1c** as well as steric demands of ^tBu groups and methyl groups of the mesityl group and the Cp⁺ ligand does not supply enough space for the η²(C)-coordination of TCNE; however, the smaller N≡C group in TCNE can be bonded to the ruthenium center in an η¹(N)-fashion.

3. Conclusion

The coordination behavior of TCNE to an electron rich metal center has been actively investigated, and there are many examples of “η²-C” complexes and several charge transfer “κ¹-N” compounds which are independently characterized. In the present paper, we have reported a reaction pathway involving one electron transfer from Ru(II) to TCNE to form the “κ¹-N” isomer having Ru(III) and TCNE⁻ moieties, which then isomerized to the “η²-C” isomer having a ruthena(IV)cyclopropane structure. To our best

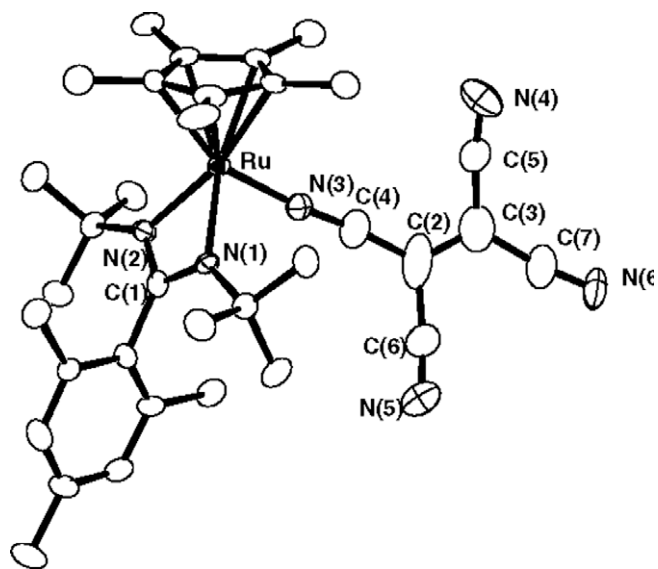


Fig. 4. The molecular structure of **2c** with 50% probability ellipsoids. The hydrogen atoms were omitted for clarity.

knowledge, there is no precedent for the stepwise coordination of TCNE to the metal center involving the “κ¹-N” to “η²-C” rearrangement, which has been unequivocally proven by crystallography and spectroscopy. The results provide fresh insight to the chemistry of a strong electron acceptor coordinating to the electron rich metal center.

4. Experimental

4.1. General

The manipulation of air and moisture sensitive organometallic compounds was carried out under a dry argon atmosphere using standard Schlenk tube techniques associated with a high-vacuum line. All solvents were distilled over appropriate drying reagents prior to use (toluene, ether, THF, hexane; Ph₂CO/Na). ¹H and ¹³C NMR spectra were recorded on a JEOL Lambda 600 or a Lambda 400 spectrometer at ambient temperature unless otherwise noted. ¹H and ¹³C NMR chemical shifts (δ values) were given in ppm relative to the solvent signal. IR spectra were recorded on a JASCO FT/IR-550 spectrometer. Melting points were measured on a Yanaco micro melting point apparatus. ESR spectrum was recorded on a JES-FA200 apparatus. Elemental analyses were performed by a Perkin Elmer 2400/CHN analyzer. Starting material, [Cp⁺RuCl]₄ was synthesized by the method reported in the literature [11].

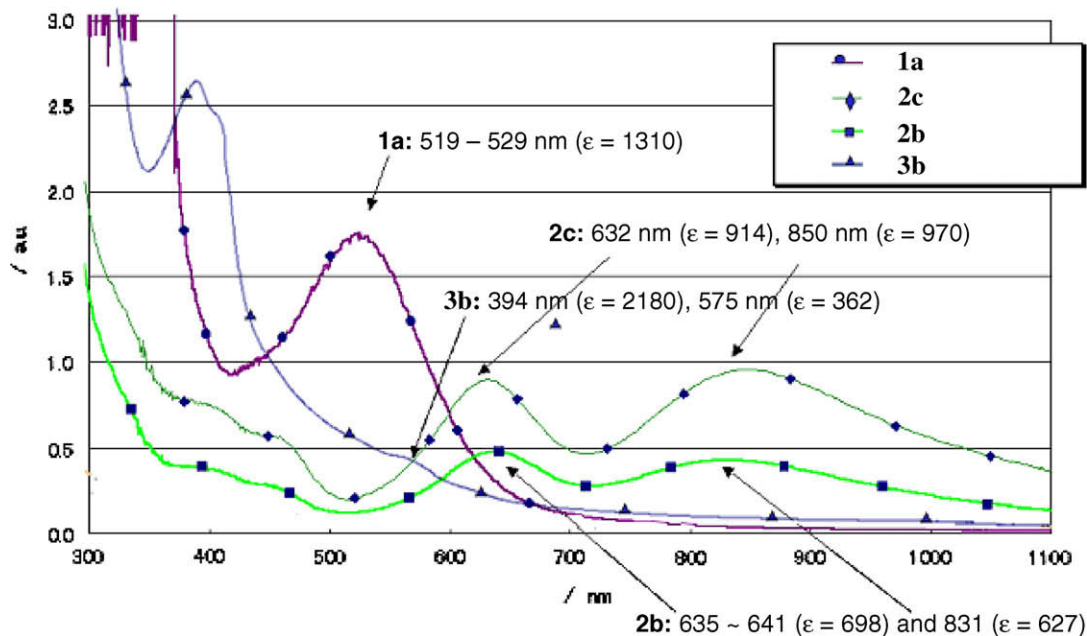


Fig. 5. UV-Vis spectra of the **1c**, **2b**, **2c**, and **3b**.

4.2. Preparation of $Cp^*Ru(\kappa^2-tBuN=C(Mes)N^tBu)$ (**1c**)

To a suspension of $[Cp^*RuCl]_4$ (174 mg, 0.16 mmol) in THF (15 mL) was added a solution of 4 equiv. of $Li^tBuN=C(Mes)N^tBu$ (180 mg, 0.64 mmol), the mixture was stirred at 60 °C for 4 h, and the resulting solution was concentrated *in vacuo*. The obtained dark purple residue was extracted with pentane twice (total 10 mL). The extracts were concentrated *in vacuo* until the volume of the solution reached ca. 2 mL. The solution was kept at –30 °C overnight to give **1c** as dark purple crystals in 98% yield (319 mg). M.p. 122 °C (dec). 1H NMR (600 MHz, THF- d_8 , r.t.): δ 1.16 (s, 18H, CH_3 of tBu), 1.69 (s, 15H, CH_3 of Cp^*), 2.20 (s, 3H, *p*- CH_3 of mesityl), 2.21 (s, 6H, *o*- CH_3 of mesityl), 2.36 (s, 6H, CH_3 of xylyl), 6.75 (s, 2H, Ph). $^{13}C\{^1H\}$ NMR (150 MHz, THF- d_8 , r.t.): δ 12.4 (s, $C_5(CH_3)_5$), 21.1 (s, *p*- CH_3 of mesityl), 22.7 (s, *o*- CH_3 of mesityl), 32.1 (s, $C(CH_3)_3$), 54.5 (s, $C(CH_3)_3$), 71.4 (s, $C_5(CH_3)_5$), 128.3, 128.6, 135.6, 138.2 (Ph), 158.9(NCN). UV-Vis (THF; λ_{max} , nm; ϵ , $M^{-1} cm^{-1}$): 519 - 529 (1310). Anal. Calc. for $C_{28}H_{44}N_2Ru$: C, 65.96; H, 8.70; N, 5.50. Found: C, 65.70; H, 8.70; N, 5.44%.

4.3. Preparation of $Cp^*Ru(\kappa^2-tBuN=C(Mes)N^tBu)(\kappa^1(N)-TCNE)$ (**2c**)

In a 50 mL Schlenk tube were placed complex **1** (53 mg, 0.1 mmol) and TCNE (13 mg, 0.1 mmol) in THF (10 mL). The resulting solution was stirred for 4 h at r.t., during which the initial dark purple solution turned dark green. The mixture was filtered through a pad of celite, then volatiles were removed *in vacuo*. The remaining dark green solid was dissolved in toluene (20 mL). The solution was concentrated to the volume of 2–3 mL, and cooled at –30 °C. Dark green crystals of **2a** were obtained in 94% yield (62 mg). M.p. 199 °C (dec). 1H NMR (600 MHz, THF- d_8 , r.t.): δ 0.68 (s, 18H, CH_3 of tBu), 1.87 (s, 15H, CH_3 of Cp^*), 1.86 (s, 3H, *o*- CH_3 of mesityl), 2.32 (s, 3H, *p*- CH_3 of mesityl), 2.50 (s, 3H, *o*- CH_3 of mesityl), 6.83 (s, 1H, Ph), 7.14 (s, 1H, Ph). $^{13}C\{^1H\}$ NMR (150 MHz, THF- d_8 , r.t.): δ 11.3 (s, $C_5(CH_3)_5$), 20.9 (s, *o*- CH_3 of mesityl), 21.2 (s, *p*- CH_3 of mesityl), 25.4 (s, *o*- CH_3 of mesityl), 35.5 (s, $C(CH_3)_3$), 57.9 (s, $C(CH_3)_3$), 106.7 (s, $C_5(CH_3)_5$), 128.4, 129.3, 136.2, 138.4, 138.7, 139.6 (Ph),

166.7(NCN). IR (KBr): $\nu_{C\equiv N}$ (cm^{-1}) = 2215, 2192, 2110 (s). UV-Vis (THF; λ_{max} , nm; ϵ , $M^{-1} cm^{-1}$): 632 (914), 850 (970). Anal. Calc. for $C_{34}H_{44}N_6Ru$: C, 64.02; H, 6.95; N, 13.17. Found: C, 63.76; H, 6.88; N, 13.08%.

4.4. Reaction of $Cp^*Ru(\kappa^2-tBuN=C(Ph)N^tBu)$ (**1b**) with TCNE to form **3b**

In a 50 mL Schlenk tube were placed complex **1** (48 mg, 0.1 mmol) and TCNE (13 mg, 0.1 mmol) in THF (10 mL). The resulting solution was stirred for 6 h at r.t., during which the initial dark purple solution first turned dark green, then dark brown. The solution was filtered through a pad of celite, then the solvent was removed *in vacuo*. The remaining dark brown solid was dissolved in toluene (20 mL). The solution was concentrated to the volume of 2–3 mL, and cooled at –30 °C. Dark brown crystals of **3b** were obtained in 89% yield (54 mg). M.p. 147 °C (dec). 1H NMR (600 MHz, THF- d_8 , r.t.): δ 1.13 (s, 18H, CH_3 of tBu), 1.87 (s, 15H, CH_3 of Cp^*), 7.28–7.36 (m, 3H, Ph), 7.33–7.45 (m, 1H, Ph), 7.62–7.68 (m, 1H, Ph). $^{13}C\{^1H\}$ NMR (150 MHz, THF- d_8 , r.t.): δ 10.5 (s, $C_5(CH_3)_5$), 18.8 (CCN), 35.6 (s, $C(CH_3)_3$), 58.5 (s, $C(CH_3)_3$), 105.9 (s, $C_5(CH_3)_5$), 119.3, 120.6 (C \equiv N), 127.9, 128.2, 130.7, 131.3, 134.2, 140.6 (Ph), 179.8 (NCN). IR (KBr): $\nu_{C\equiv N}$ (cm^{-1}) = 2229 (s), 2211 (s). UV-Vis (THF; λ_{max} , nm; ϵ , $M^{-1} cm^{-1}$): 635–641 (698), 831 (627). Anal. Calc. for $C_{31}H_{38}N_6Ru$: C, 62.50; H, 6.49; N, 14.11. Found: C, 62.44; H, 6.35; N, 14.20%.

4.5. X-ray data collection and reduction

X-ray crystallography was performed on a Rigaku Saturn CCD area detector in the case of **1c**, and on a Rigaku RAXIS RAPID imaging plate diffraction meter in the case of **2c** with graphite monochromated Mo $K\alpha$ radiation ($\lambda = 0.71070 \text{ \AA}$). The data were collected at 123(2) K using ω scan in the θ range of $2.2 \leq \theta \leq 27.5^\circ$ (**1c**) and $3.1 \leq \theta \leq 27.5^\circ$ (**2c**). The data obtained were processed using Crystal-Clear (Rigaku) on a Pentium computer, and were corrected for Lorentz and polarization effects. The structures were solved by direct methods [12], and expanded using Fourier techniques [13]. The non-hydrogen atoms were refined anisotropically.

ically except for the disordered solvent atoms (toluene for **2c**). Hydrogen atoms were refined using the riding model. The final cycle of full-matrix least-squares refinement on F^2 was based on 5781 observed reflections and 324 variable parameters for **1c**, 8527 observed reflections and 474 variable parameters for **2c**. Neutral atom scattering factors were taken from Cromer and Waber [14]. All calculations were performed using the CrystalStructure [15,16] crystallographic software package. Details of final refinement as well as the bond lengths and angles are summarized in the supporting information, and the numbering scheme employed is also shown in the supporting information, which were drawn with ORTEP at 50% probability ellipsoid.

Acknowledgements

This work was supported by Grant-in-Aid for Science Research on Priority Areas (No. 18064014, Synergy of Elements) from Ministry of Education, Culture, Sports, Science and Technology, Japan.

Appendix A. Supplementary material

Supplementary data associated with this article can be found, in the online version, at doi:10.1016/j.jorganchem.2008.12.030.

References

- [1] (a) W. Kaim, M. Moscherosch, *Coord. Chem. Rev.* 129 (1994) 157; (b) D. de Caro, C. Faulmann, L. Valade, *Chem. Eur. J.* 13 (2007) 1650; (c) J.S. Miller, A.J. Epstein, W.M. Reiff, *Chem. Rev.* 88 (1988) 201; (d) J.S. Miller, A.J. Epstein, W.M. Reiff, *Acc. Chem. Res.* 21 (1988) 114.
- [2] R.H. Crabtree (Ed.), *The Organometallic Chemistry of the Transition Metals*, 4th ed., Wiley, New York, 2001, p. 125 (Chapter 3).
- [3] (a) R.M. Rettig, R.M. Wing, *Inorg. Chem.* 8 (1969) 2685; (b) H. Braunwarth, F. Hutter, L. Zsolnai, *J. Organomet. Chem.* 372 (1989) C23.
- [4] (a) For example, see: G. Wang, H. Zhu, J. Fan, C. Slebodnick, G.T. Yee, *Inorg. Chem.* 45 (2006) 1406; (b) F. Baumann, M. Heilmann, W. Matheis, A. Schulz, W. Kaim, J. Jordanov, *J. Organomet. Chem.* 251 (1996) 236; (c) M.J. Macazaga, M.S. Delgado, J.R. Masaguer, *J. Organomet. Chem.* 310 (1986) 249; (d) M.J. Macazaga, M.S. Delgado, J.R. Masaguer, *J. Organomet. Chem.* 299 (1986) 377; (e) S.D. Ittel, C.A. Tolman, P.J. Krusic, A.D. English, J.P. Jesson, *Inorg. Chem.* 17 (1978) 3432; (f) S.I. Amer, T.P. Dasgupta, P.M. Henry, *Inorg. Chem.* 22 (1983) 1970; (g) B. Olbrich-Duessner, W. Kaim, R. Gross-Lannert, *Inorg. Chem.* 29 (1990) 5046.
- [5] (a) For instance, Kaim et al. have reported the excellent works concerning with isomerization of TCNE from $\eta^2(\text{C})$ -TCNE to $\eta^1(\text{N})$ -coordination achieved by the reduction of the parent $\eta^2(\text{C})$ -TCNE complexes electrochemically or chemically. For further details of the rearrangement of TCNE from $\eta^2(\text{C})$ - to $\eta^1(\text{N})$ -coordination, see: T. Roth, W. Kaim, *Inorg. Chem.* 31 (1992) 1930; (b) B. Olbrich-Duessner, R. Gross, W. Kaim, *J. Organomet. Chem.* 366 (1989) 155; (c) B. Olbrich-Duessner, W. Kaim, R. Gross-Lannert, *Inorg. Chem.* 28 (1989) 3113; (d) T. van Houwelingen, D.J. Stufkens, A. Oskam, *Coord. Chem. Rev.* 111 (1991) 325.
- [6] Y. Yamaguchi, H. Nagashima, *Organometallics* 19 (2000) 725.
- [7] (a) H. Nagashima, H. Kondo, T. Hayashida, Y. Yamaguchi, M. Gondo, S. Masuda, K. Miyazaki, K. Matsubara, K. Kirchner, *Coord. Chem. Rev.* 245 (2003) 177; (b) H. Nagashima, M. Gondo, S. Masuda, H. Kondo, Y. Yamaguchi, K. Matsubara, *Chem. Commun.* (2003) 442; (c) T. Hayashida, H. Nagashima, *Organometallics* 21 (2002) 3884; (d) T. Hayashida, Y. Yamaguchi, K. Kirchner, H. Nagashima, *Chem. Lett.* (2001) 954; (e) T. Hayashida, K. Miyazaki, Y. Yamaguchi, H. Nagashima, *J. Organomet. Chem.* 634 (2001) 167; (f) H. Kondo, A. Kageyama, Y. Yamaguchi, M. Haga, K. Kirchner, H. Nagashima, *Bull. Chem. Soc. Jpn.* 74 (2001) 1927; (g) T. Hayashida, H. Nagashima, *Organometallics* 20 (2001) 4996; (h) H. Kondo, Y. Yamaguchi, H. Nagashima, *Chem. Commun.* (2000) 1075; (i) T. Hayashida, H. Kondo, J. Terasawa, K. Kirchner, Y. Sunada, H. Nagashima, *J. Organomet. Chem.* 692 (2007) 382.
- [8] (a) D.N. Dhar, *Chem. Rev.* 67 (1967) 611; (b) J.S. Miller, *Angew. Chem., Int. Ed.* 45 (2006) 2508.
- [9] [a] see ref (6d); (b) T.J. Johnson, K. Folting, W.E. Streib, J.D. Martin, J.C. Huffman, S.A. Jackson, O. Eisenstein, K.G. Caulton, *Inorg. Chem.* 34 (1995) 488; (c) K. Mashima, H. Kaneyoshi, S. Kaneko, A. Mikami, K. Tani, A. Nakamura, *Organometallics* 16 (1997) 1016; (d) E.J. Derrah, D.A. Pantazis, R. McDonald, L. Rosenberg, *Organometallics* 26 (2007) 1473; (e) W.M. Cheung, Q.-F. Zhang, I.D. Williams, W.H. Leung, *Inorg. Chim. Acta* 359 (2006) 782; (f) V.N. Sapunov, R. Schmid, K. Kirchner, H. Nagashima, *Coord. Chem. Rev.* 238–239 (2003) 363; (g) C. Gemel, J.C. Huffman, K.G. Caulton, K. Mauthner, K. Kirchner, *J. Organomet. Chem.* 593–594 (2000) 342; (h) C. Gemel, V.N. Sapunov, K. Mereiter, M. Ferencic, R. Schmid, K. Kirchner, *Inorg. Chim. Acta* 286 (1999) 114; (i) C. Gemel, K. Mereiter, R. Schmid, K. Kirchner, *Organometallics* 16 (1997) 5601; (j) U. Koelle, *Chem. Rev.* 98 (1998) 1313; (k) C.D. Tagge, R.G. Bergman, *J. Am. Chem. Soc.* 118 (1996) 6908.
- [10] Diamagnetic nature of **2c** can be interpreted in terms of the antiferromagnetic coupling between TCNE⁻ and Ru(III) center. See Refs. [1a,3a,4c,8a].
- [11] P.J. Fagan, M.D. Ward, J.C. Calabrese, *J. Am. Chem. Soc.* 111 (1989) 1698.
- [12] (a) G.M. Sheldrick, *SHELX97*, 1997.; (b) A. Altomare, M.C. Burla, M. Camalli, G. Cascarano, A. Guagliardi, A. Moliterni, G. Polidori, R. Spagna, *SIR97*, 1999.
- [13] P.T. Beurskens, G. Admiraal, G. Beurskens, W.P. Bosman, R. de Gelder, R. Israel, J.M.M. Smits, The *DIRDIF-99* Program System; Technical Report of the Crystallography Laboratory, University of Nijmegen, Nijmegen, The Netherlands, 1999.
- [14] D.T. Cromer, J.T. Waber, *International Tables for X-ray Crystallography*, vol. 4, Kynoch Press, Birmingham, UK, 1974.
- [15] CrystalStructure 3.8.0: Crystal Structure Analysis Package; Package, Rigaku and Rigaku/MSC, 9009 New Trails Dr, The Woodlands TX 77381 USA, 2000–2006.
- [16] J.R. Carruthers, J.S. Rollett, P.W. Betteridge, D. Kinna, L. Pearce, A. Larsen, E. Gabe, *CRYSTALS Issue 11*, Chemical Crystallography Laboratory, Oxford, UK, 1999.